

RESEARCH PAPER



In silico identification of novel SARS-COV-2 2'-O-methyltransferase (nsp16) inhibitors: structure-based virtual screening, molecular dynamics simulation and MM-PBSA approaches

Mahmoud A. El Hassab^a, Tamer M. Ibrahim^b, Sara T. Al-Rashood^c, Amal Alharbi^c, Razan O. Eskandrani^c and Wagdy M. Eldehna^b

^aDepartment of Pharmaceutical Chemistry, Faculty of Pharmacy, Badr University in Cairo (BUC), Badr City, Egypt; ^bDepartment of Pharmaceutical Chemistry, Faculty of Pharmacy, Kafrelsheikh University, Kafrelsheikh, Egypt; ^cDepartment of Pharmaceutical Chemistry, College of Pharmacy, King Saud University, Riyadh, Saudi Arabia

ABSTRACT

The novel coronavirus disease COVID-19, caused by the virus SARS CoV-2, has exerted a significant unprecedented economic and medical crisis, in addition to its impact on the daily life and health care systems all over the world. Regrettably, no vaccines or drugs are currently available for this new critical emerging human disease. Joining the global fight against COVID-19, in this study we aim at identifying a potential novel inhibitor for SARS COV-2 2'-O-methyltransferase (nsp16) which is one of the most attractive targets in the virus life cycle, responsible for the viral RNA protection *via* a cap formation process. Firstly, nsp16 enzyme bound to Sinefungin was retrieved from the protein data bank (PDB ID: 6WKQ), then, a 3D pharmacophore model was constructed to be applied to screen 48 Million drug-like compounds of the Zinc database. This resulted in only 24 compounds which were subsequently docked into the enzyme. The best four score-ordered hits from the docking outcome exhibited better scores compared to Sinefungin. Finally, three molecular dynamics (MD) simulation experiments for 150 ns were carried out as a refinement step for our proposed approach. The MD and MM-PBSA outputs revealed compound **11** as the best potential nsp16 inhibitor herein identified, as it displayed a better stability and average binding free energy for the ligand-enzyme complex compared to Sinefungin.

ARTICLE HISTORY

Received 8 November 2020
Revised 6 December 2020
Accepted 27 January 2021

KEYWORDS

SARS COV-2 2'-O-methyltransferase (nsp16) Inhibitor; 3D pharmacophore; molecular dynamics; MM-PBSA calculations; COVID-19 therapies





Introduction


Since 11th March 2020, COVID-19 caused by severe acute respiratory syndrome (SARS-COV-2) virus was declared by the WHO as a pandemic disease. The virus is extremely dangerous affecting more than 200 countries with 46 202 728 confirmed cases and 1,197,739 deaths by the 31th of October 2020. The available treatment protocol for COVID-19 infection is limited to a few drugs that at their maximum efficacy may only reduce the symptoms of the infection¹. Thus, it is an urgent need to develop a specific treatment for the COVID-19 infection using various drug discovery means. There are many approved direct acting antiviral agents (DAA), which have significantly reduced or diminished the viral load and have achieved great therapeutic outcomes in the treatment of viruses such as Hepatitis Virus B, C, or AIDS. Each of these DAAs has a specific target in the virus life cycle for instance, Simeprevir acts on HCV NS3 protease while Elvitegravir acts on HIV integrase^{2,3}. So, developing a specific potent DAA for COVID-19 infection could be achieved only if full understanding of the function and structural features of essential targets is provided.

SARS-COV2 transmission could be conveyed through different modes, e.g. mainly through respiratory droplets, and like other

respiratory viruses when exposing to sneezing or coughing from COVID-19 patients, through faces, and close contact less than 2 metres⁴. The crown-like virus has a genome of ~30000 nucleotides in length which encodes several proteins. Four of them are structural proteins namely, Nucleocapsid (N) protein, Membrane (M) protein, Spike (S) protein and Envelop (E) protein and the rest of the encoded polyprotein is non-structural proteins (nsp) that are essentials in the virus replication cycle^{5,6}.

The life cycle of the virus starts after attaching its spike protein to the human angiotensin converting enzyme 2 (ACE2) receptors present at the surface of numerous cells like those of lungs and GIT. Then, the fusion peptide is released after proteolytic cleavages of the Spike protein by host proteases. This is followed by a cascade of cellular processes that end by virus entry into the cytoplasm. After that, the virus is uncoated releasing its single-stranded RNA genome into cytoplasm where the replication and transcription take place by the aid of the virus several non-structural proteins. Finally, the resulting proteins from the replication and transcription processes are assembled into new virions ready to infect new cells⁵⁻⁷. Many essential targets in the described life cycle had been proposed as potential for developing specific DAAs for COVID-19 infection such as the non-structural protein 12

CONTACT Wagdy M. Eldehna  wagdy2000@gmail.com  Department of Pharmaceutical Chemistry, Faculty of Pharmacy, Kafrelsheikh University, P.O. Box 33516, Kafrelsheikh, Egypt; Mahmoud A. El Hassab  mahmoud65582@pharm.tanta.edu.eg  Department of Pharmaceutical Chemistry, Faculty of Pharmacy, Badr University in Cairo (BUC), Badr City, Cairo, Egypt

 Supplemental data for this article can be accessed [here](#).

© 2021 The Author(s). Published by Informa UK Limited, trading as Taylor & Francis Group.

This is an Open Access article distributed under the terms of the Creative Commons Attribution License (<http://creativecommons.org/licenses/by/4.0/>), which permits unrestricted use, distribution, and reproduction in any medium, provided the original work is properly cited.

(nsp12); RNA Dependent RNA Polymerase (RdRp) which is essential in replicating the virus genome. Also, the 3C-like protease (3CL^{Pro}) and Papin like protease (PL^{Pro}) are two important targets that play a crucial role in the SARS-COV-2 replication cycle by processing the resulting polyprotein from the transcription stage into functioning subunits. Moreover, many studies had been reported aiming to prevent the virus entry by blocking the attachment between the Spike protein and the human angiotensin converting enzyme 2 receptor (ACE2)^{8–10}.

Another promising target that worth detailed mentioning is the SARS COV-2 2'-O-methyltransferase (nsp16), which is an important enzyme for the virus survival. The role of the SARS COV-2 2'-O-methyltransferase (nsp16) is to protect the viral RNA from the cellular innate immunity through participation in the formation of a specific arrangement at the 5' end of the RNA molecule that consists of *N*-methylated guanosine triphosphate and C2'-O-methyl-ribosyladenine. This arrangement is called RNA cap that resembles the native mRNA of the host cells, stabilises the RNA, and ensures effective process of its translation. The cap formation starts when 5'-RNA triphosphatase removes a γ -phosphate from a 5'-triphosphate end of the nascent RNA. Then, to the formed 5'-diphosphate end of RNA, guanylyltransferase attaches a guanosine monophosphate (GMP). At last, two steps of methylation are executed by two distinct enzymes, nsp14 that adds a methyl group at *N*-7 of the GTP nucleobase (*N*-7 methyltransferase) and nsp16 that adds a methyl group at C2'-O of the next nucleotide^{11,12}. This process is crucial for RNA stability, preventing its degradation by the host¹³. The process and importance of cap formation reveals that SARS COV-2 2'-O-methyltransferase (nsp16) is a very promising target and its targeting could result in effective inhibition of COVID-19 infection^{13,14}. We had successfully reported the ability of Structure-Based Drug Discovery (SBDD) in the identification of novel potential inhibitor for SARS-COV-2 Polymerase enzyme¹⁵.

Herein in this study, we report the application of Structure-Based Virtual Screening (SBVS) strategies with the prime goal of identification of novel potential inhibitors for SARS COV-2 2'-O-methyltransferase (nsp16) utilising integrated Structure-based virtual screening, molecular docking, molecular dynamics simulation and MM-PBSA approaches, as illustrated in (Figure 1).

Materials and methods

3D Pharmacophore generation

The crystal structure of the SARS COV-2 2'-O-methyltransferase (nsp16) in complex with the pan-methyl-transferase inhibitor Sinefungin was retrieved from the protein data bank; PDB ID: 6WKQ. The retrieved complex was energy minimised by employing the steepest descent minimisation algorithm with a maximum of 50,000 steps and <10.0 kJ/mol force, then the energy minimised complex was equilibrated for 10 ns to elucidate the most stable conformation and to prepare the complex for further *in silico* experiments see *Molecular dynamic section*. The interaction diagram between Sinefungin and the minimised and equilibrated SARS COV-2 2'-O-methyltransferase (nsp16) was generated by Discovery Studio Visualiser 2020 to determine the types and number of the formed interactions, as well as the functional groups in Sinefungin responsible for those interactions (Figure 2). MOE 2019 was implemented to generate 3D pharmacophore features according to the interacting function groups of Sinefungin with its target¹⁶. Thereafter, the generated pharmacophore was used to screen the ZINC15 database (~48 M compounds) aiming to identify potential potent inhibitors for SARS COV-2 2'-O-methyltransferase (nsp16).

Database generation and optimisation for pharmacophore screening

The Zinc Drug-like library (nearly 48 million compounds, available at <http://zinc.docking.org>) was downloaded as smiles files and then converted into single database file with extension mdb by MOE suite (MOE, 2019 (<https://www.chemcomp.com>)). AMBER14: EHT force field was used for energy minimisation of the generated compound library using steepest descent algorithm until RMS gradient of 0.1 Kcal/Mol/A is reached¹⁶.

Virtual screening

A two-stage virtual screening approach, combining pharmacophore-based virtual screening and docking-based virtual screening

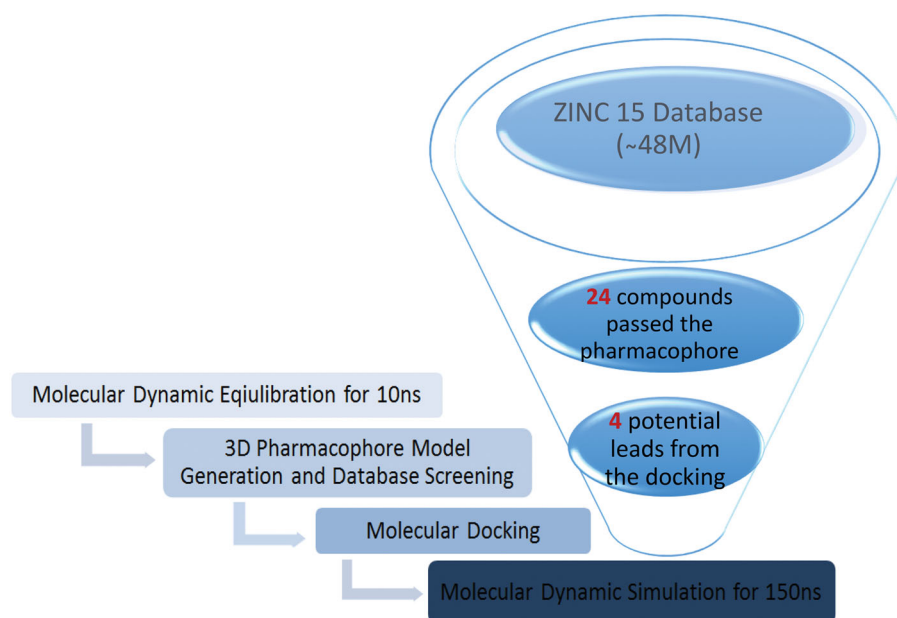


Figure 1. The virtual screening steps and the implemented protocol for the identification of potential inhibitors for SARS COV-2 2'-O-methyltransferase (nsp16).

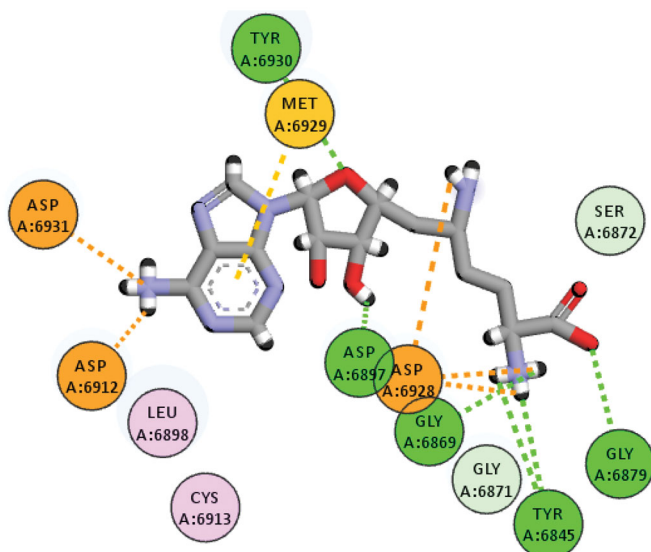


Figure 2. 2D Binding of sinefungine within SARS-COV-2 2'-O-methyltransferase binding site after 10 ns of equilibration.

was employed to identify potential active compounds against nsp16.

Pharmacophore-based virtual screening

The prepared compounds library of the Zinc database was screened using the constructed 3D pharmacophore model using MOE 2015 pharmacophore wizard^{17,18}. After a series of trials; all the screened compounds were required to match five of the features in the pharmacophore hypothesis. The distance matching tolerance was designated to 2.0 Å. A fitness score was used to rank the database hits based on their RMSD with the hypothesis involving site matching, vector alignments and volume terms. Compounds that passed the pharmacophore filter were further screened through docking-based virtual screening.

Docking-based virtual screening

This section aims to identify the most potential active compounds resulting from the pharmacophore search as well as predicting their possible mode of binding to the SARS COV-2 2'-o-methyltransferase (nsp16). To provide a rough validation of the docking protocol used, we performed a pose-retrieval docking experiments for the X-ray coordinates of Sinefungin in the binding site of nsp16, for two scenarios, in presence and in absence of water molecules of the binding site. The calculated RMSD values were 0.53 and 0.25 Å in the NW-docking (docking without water) and the W-docking (docking with water) respectively, therefore the water molecules were removed in docking procedure to increase the diversity of selected compounds¹⁹ (Figure S1, Supplementary information). AutoDock Vina software was used to conduct the previous step in addition to the successful candidates from the pharmacophore search. MGL tools 1.5.7 was implemented to prepare the equilibrated nsp16, Sinefungin and the successful candidates from the pharmacophore search were converted into pdbqt format; a prerequisite for Vina Autodock software^{20,21}. The active site was determined by generating a grid box sized 24 × 24 × 24 Å³ surrounding the binding site of Sinefungin. The best candidates were selected for further analysis based on the docking and

the interaction diagram generated by Discovery Studio Visualiser²².

Molecular dynamics

We conducted three molecular dynamic simulations experiments to support our concept of design and to validate the predicting binding mode of compound **11**. Two experiments were conducted for SARS COV-2 2'-o-methyltransferase (nsp16) complex with Sinefungin and compound **11**, respectively, while another one was for the free unbound SARS COV-2 nps16. The latest version of Groningen Machine for Chemical Simulations (GROMACS 2020.3) was employed to conduct the entire MD simulation experiments²³. The ligand topologies were obtained by the CHARMM General Force Field CGENFF server and converted into the desired gromacs format using the "cgenff_charmm2gmx_py3_nx2.py" script, while the receptor topology was obtained by the "pdb2gmx" script²⁴. The generated ligand topologies were rejoined to the processed receptor structure to construct the ligand-protein complex. All the processed complexes were energy minimised under GROMOS96 43a1 force field²⁵. After that, those complexes were solvated with a single point charge (SPC) water model to add water molecules to the cubic simulation boxes.

System neutralisation of the net charges was done by adding counter-ions using the "gmx genion" script. Energy minimisation of the unbound enzyme and the two complexes was achieved by employing the steepest descent minimisation algorithm with a maximum of 50,000 steps and <10.0 kJ/mol force. Then, the solvated energy minimised structures were equilibrated with two consecutive steps. Firstly, NVT ensemble with constant number of particles, volume and temperature (310 K) was done for 2 ns followed by NPT ensemble with constant number of particles, pressure and temperature for 8 ns. In the two systems, only the solvent molecules were allowed for free movement to ensure its equilibration in the system while other atoms were restrained. The long range electrostatic interactions were obtained by the particle mesh Eshwald method with a 12 Å cut-off and 12 Å Fourier spacing²⁶. Finally, the three well-equilibrated systems (one empty protein and two protein-ligand complexes) were then entered the production stage without any restrains for 150 ns with a time step of 2 fs, and after every 10 ps the structural coordinates were saved to retrieve 15000 frames for each processed complex. The root mean square deviation (RMSD) was calculated from the generated trajectories of the MD simulations as well as the distances of the formed hydrogen bonds between the receptor and the ligands by various scripts of GROMACS.

MM-PBSA calculation

An important feature of MD simulations and thermodynamic calculations coupling is the ability to measure the binding free energy of a protein-ligand complex. Combining molecular Mechanic/Poisson-Boltzmann Surface Area (MM-PBSA) alongside MD simulations has been reported in successful calculation of the binding free energy of protein and ligand complexes via the application of the following equation:

$$\Delta G_{\text{(Binding)}} = G_{\text{(Complex)}} - G_{\text{(Receptor)}} - G_{\text{(Ligand)}}$$

Where, $G_{\text{(complex)}}$ is the total free energy of the protein – ligand complex and $G_{\text{(receptor)}}$ and $G_{\text{(ligand)}}$ are total free energies of the isolated protein and ligand in solvent, respectively. The total free energy of any of the three mentioned entities (complex or receptor or ligand) could be calculated from

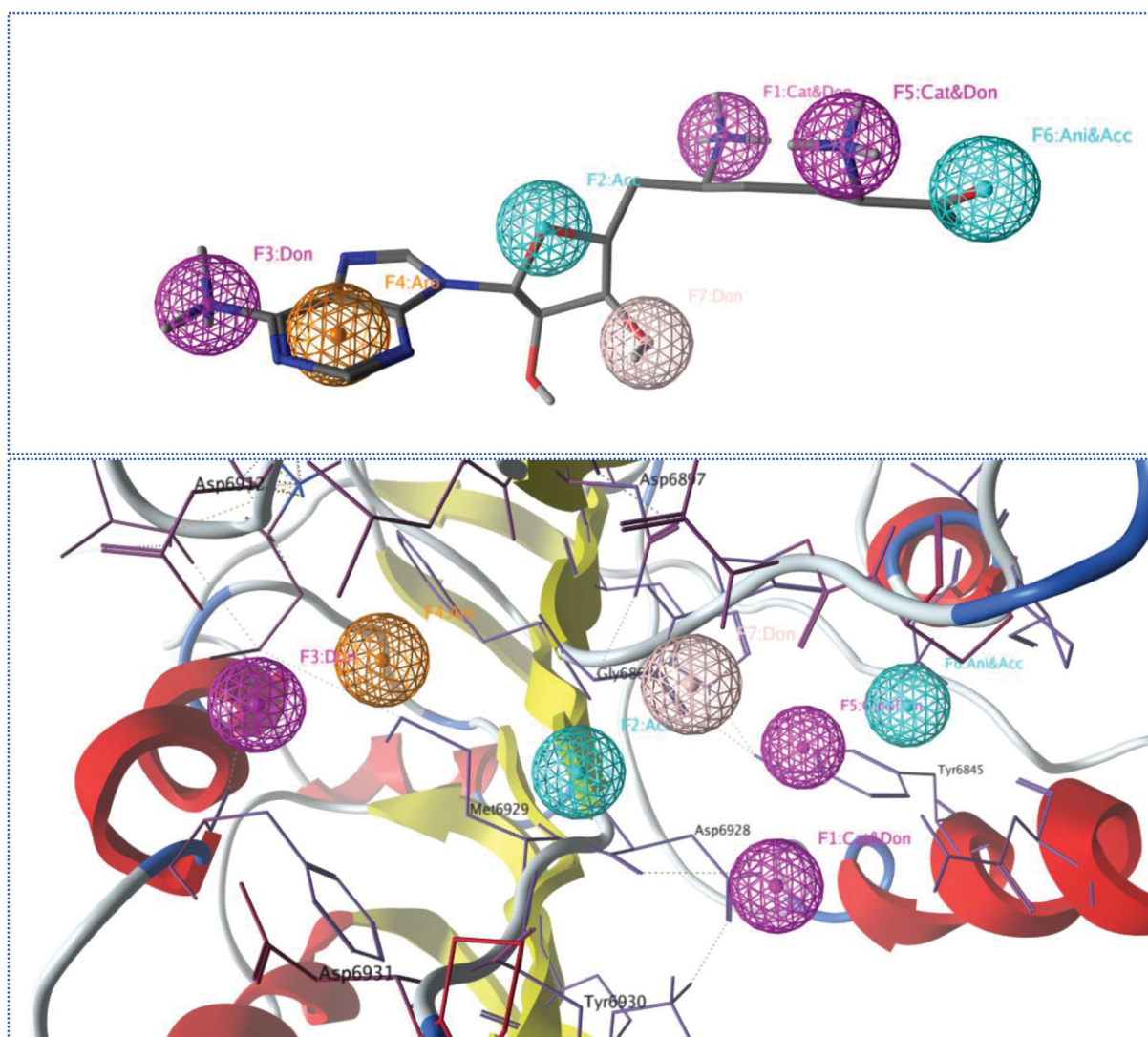


Figure 3. The generated 3D pharmacophore; Blue spheres represent acceptor features, pale pink sphere represents donor features, dark pink spheres represent cationic donor features and orange sphere represents aromatic feature.

its molecular mechanics potential energy plus the energy of solvation. Thus, the “g_mmpbsa”²⁷ package of GROMACS was used to perform MM-PBSA calculations through all the MD trajectories.

Results and discussion

3D Pharmacophore

Analysis of SARS-COV-2 2'-O-methyltransferase (nsp16) crystal structure that contains Sinefungine as a co-crystallized ligand revealed numerous numbers and types of interactions between Sinefungine and its corresponding binding domain. Converting all those interactions to 3D pharmacophore features is practically inapplicable and the virtual screening will fail to find any ligand (Figure S2, Supplementary Information). Indeed, not all the formed interactions between a ligand and its target are responsible directly for the ligand activity, otherwise only stable interactions may have the most significant contribution to the activity. Accordingly, the crystal structure was energy minimised and equilibrated for 10 ns to elucidate such stable interactions and then convert them to 3D pharmacophore features. In the equilibrated structure,

Sinefungine was able to maintain strong pattern of interaction through seven function groups, (Figure 2).

The interacting atoms within each functional group in Sinefungine, as well as, the interaction types enabled us to generate a 3D pharmacophore of four features and seven components (Figure 3). Namely, the pharmacophore model consisted of three cationic donor features to attract the negative charge on (Asp6912, Asp6928 and Asp6931), one donor feature to interact with (Asp6897), two acceptor features to interact with (Gly6879 and Tyr6930), and an aromatic feature to interact with (Met6929). The generated pharmacophore was used to screen the ZINC15 drug-like database and the successful compounds were required to match all the features. Unfortunately, no compound was able to match all the features and the same happened when compounds were required to match six of the seven features. Thus, compounds were asked to match at least five of the seven features and this resulted in 24 potential lead compounds (Supplementary Information) that may act as SARS COV-2 2'-O-methyltransferase (nsp16) inhibitors. Thereafter, these potential lead compounds were further evaluated against SARS COV-2 2'-O-methyltransferase (nsp16) *via* molecular docking studies.

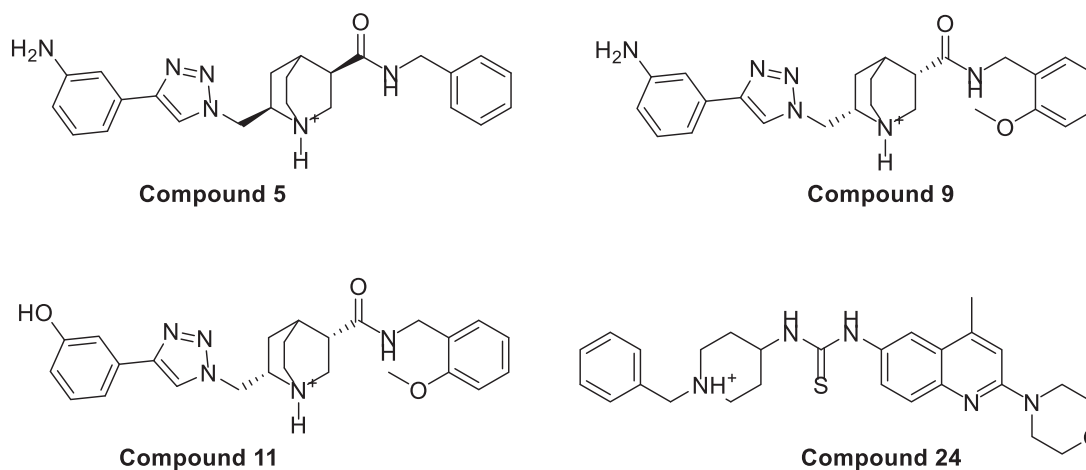


Figure 4. Chemical structures for compounds 5, 9, 11 and 24.

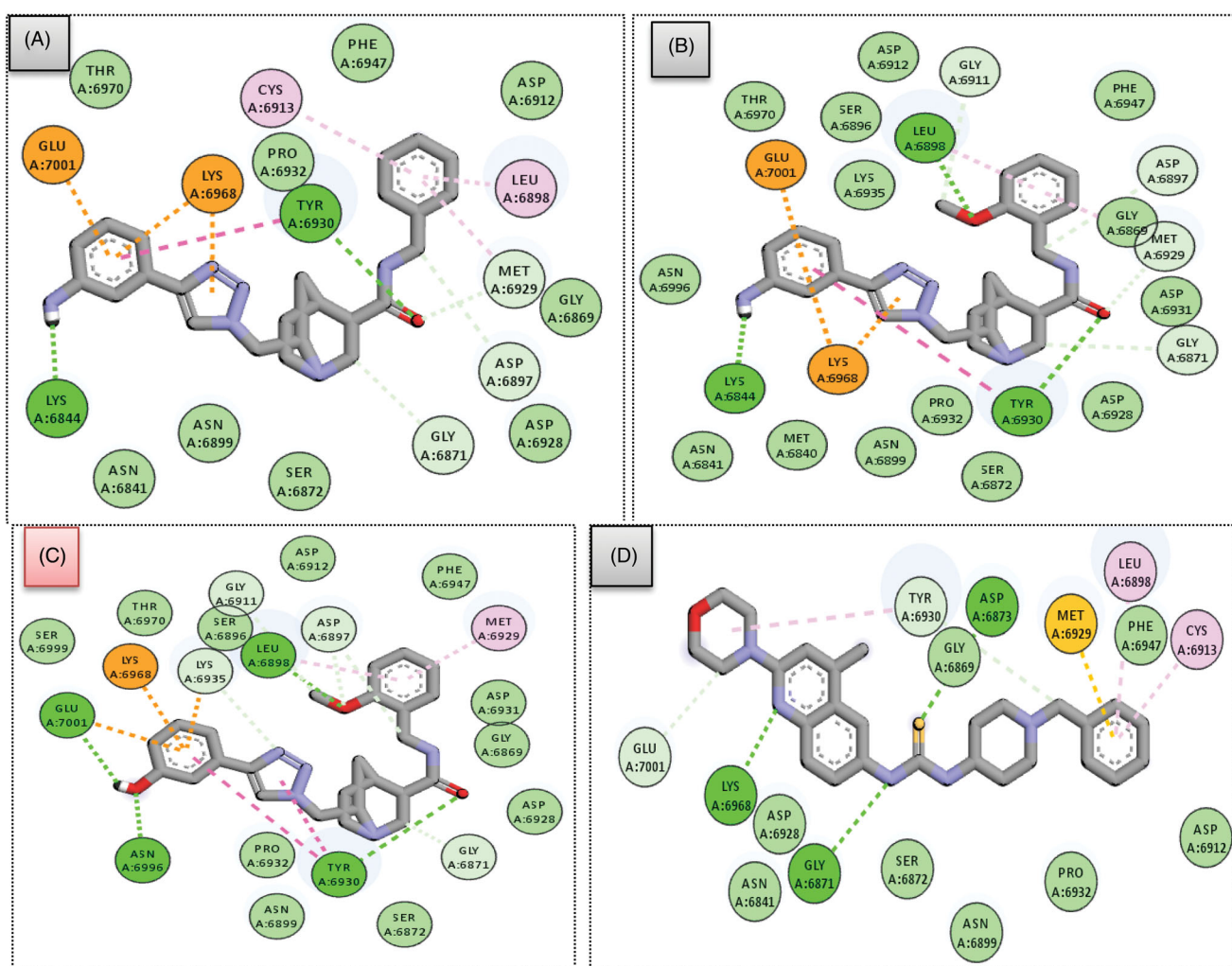


Figure 5. 2D interactions of compounds 5 (A), 9 (B), 11 (C) and 24 (D) within SARS-CoV-2 2'-O-methyltransferase binding site.

Docking

In Computer-aided drug design studies, docking strategy stands out as one of the most important techniques providing many useful applications, including the prediction of the binding mode between a ligand and its target, ranking a library of compounds

based on their docking scores and correlating those scores with potential activity. Also, docking has a valuable role in characterising the effect of certain amino acids mutations on the activity profile of the ligands. Moreover, visualising the interaction images resulting from docking software gives insights and guides for the optimisation of the existing ligands to yield compounds with

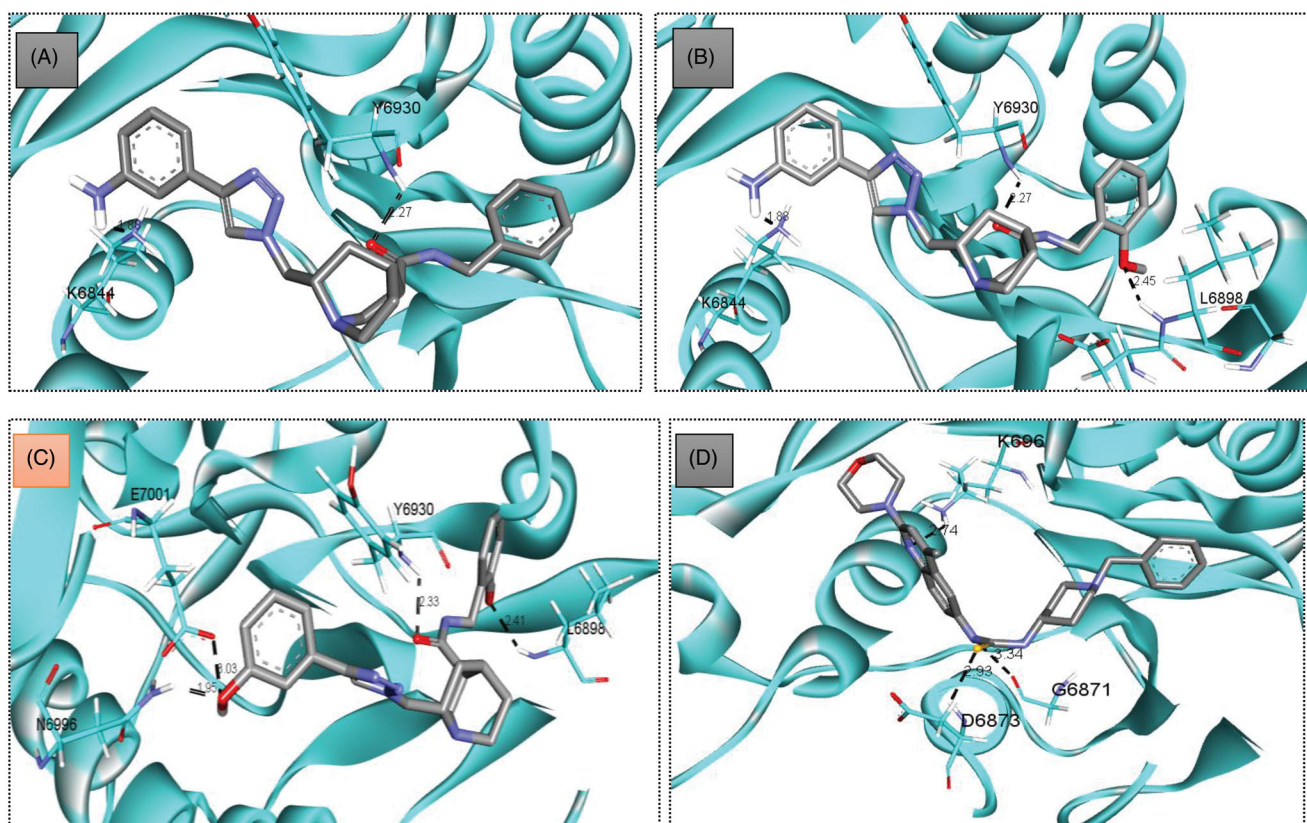


Figure 6. 3D representation for inhibitors **5** (A), **9** (B), **11** (C) and **24** (D) displaying their interactions within SARS-COV-2 2'-O-methyltransferase binding site.

better affinity. In the current study, docking was implemented to rank the successful 24 candidates from the pharmacophore search, besides predicting the plausible binding mode with their target.

Based on the results obtained from AutoDock Vina, only four compounds (**5**, **9**, **11** and **24**, Figure 4), among the 24 potential leads, were able to achieve better docking score ($S = -10.1$, -10.3 , -10.6 and -9.9 Kcal/mol, respectively) than Sinefungine ($S = -8.5$ Kcal/mol), and thus were selected for further analysis.

Compounds **5**, **9** and **11**, with the same scaffold and similar structures, displayed a similar strong pattern of interaction with their target, which indicates a valid docking approach. On the other hand, compound **24** is based on a different scaffold and thus it was oriented into the receptor in a different manner. In general, the four compounds (**5**, **9**, **11** and **24**) demonstrated a strong binding affinity with many types of interaction with the SARS-COV-2 2'-O-methyltransferase binding site (Figures 5 and 6).

In particular, methoxy-bearing compounds **9** and **11** achieved the best docking score ($S = -10.3$ and -10.6 Kcal/mol, respectively) among the four compounds. They were engaged in two hydrogen bond interactions *via* both methoxy (OCH_3) and amidic carbonyl ($\text{C}=\text{O}$) functional groups with Leu6898 and Tyr6930 amino acids, respectively (Figure 5, 6(B–C)). In addition, the primary amino group (NH_2) in compound **9** was involved in a hydrogen bond interaction with Lys6844 amino acid, whereas, the hydroxyl group (OH) in compound **11** was able to establish two hydrogen bond interactions with Asn6996 and Glu7001 amino acids.

On the other hand, compound **5** lacks the methoxy group found in compounds **11** and **9**, thus, it was able to form only two hydrogen bonds with Tyr6930 and Lys6844 *via* its amidic carbonyl ($\text{C}=\text{O}$) and primary amino group (NH_2) functional groups (Figure 5, 6(A)). Furthermore, compound **24** was involved in three hydrogen bond interactions with Gly6871, Asp6873 and Lys696, yet it

came in the last rank ($S = -9.9$ Kcal/mol) as it lacks various hydrophobic interactions achieved by the other three compounds (Figure 5, 6(D)). Table 1 summarises all the bonding interactions and distances for compounds (**5**, **9**, **11** and **24**) within SARS-COV-2 2'-O-methyltransferase binding site.

Molecular dynamics

In many computational studies of drug discovery, Molecular dynamic simulations have provided valuable assessment in identification of potential inhibitors for promising targets, studying the nature of macromolecules or interpretations of drug resistances^{28–31}. To support our protocol so far, and to provide insights on the stability of the predicted binding mode of compound **11** in the binding site of nsp16, also to identify and study the dynamic nature of the SARS COV-2 2'-O-methyltransferase (nsp16) and correlate this to the key biological role played by this enzyme in the virus life cycle, we conducted three molecular dynamic simulation experiments.

RMSD analysis and hydrogen bond monitoring

The ultimate endeavour for SARS-COV-2 2'-O-methyltransferase (nsp16) is to prevent the degradation of the viral RNA through the process of Cap formation as previously mentioned. Moreover, this enzyme should have a high degree of flexibility and dynamicity to deliver its intended function^{32,33}. So, the conducted simulation experiment for the unbound SARS-COV-2 2'-O-methyltransferase aimed to be used as a reference for comparison with the other two simulation experiments. The calculated RMSD of all the residues of the unbound enzyme reached 3.70 \AA

Table 1. Different bonding types and their distances (in Å) for compounds (**5**, **9**, **11** and **24**) within SARS-COV-2 2'-O-methyltransferase binding site

Compound	Energy Score (kcal/mol)	Interactions	Distance		
11	-10.6	Hydrogen bond with Leu6898	2.41		
		Hydrogen bond with Tyr6930	2.33		
		Hydrogen bond with Asn6996	1.95		
		Hydrogen bond with Glu7001	3.03		
		Non-classical carbon Hydrogen bond with Gly6871	3.50		
		Non-classical carbon Hydrogen bond with Asp6897	3.39		
		Non-classical carbon Hydrogen bond with Asp6897	2.54		
		Non-classical carbon Hydrogen bond with Gly6911	3.63		
		Non-classical carbon Hydrogen bond with Lys6935	2.98		
		Pi-Alkyl interaction with Leu6898	5.05		
		Pi-Alkyl interaction with Met6929	4.14		
		Pi-Pi interaction with Tyr6930	4.82		
		Pi-Pi interaction with Tyr6930	4.87		
		Pi-Anion interaction with Glu7001	3.99		
		Pi-Cation interaction with Lys6935	3.14		
		Pi-Cation interaction with Lys6996	3.84		
		9	-10.3	Hydrogen bond with Leu6898	2.45
Hydrogen bond with Tyr6930	2.27				
Hydrogen bond with Lys6844	1.88				
Non-classical carbon Hydrogen bond with Gly6871	3.56				
Non-classical carbon Hydrogen bond with Asp6897	3.39				
Non-classical carbon Hydrogen bond with Gly6911	3.68				
Non-classical carbon Hydrogen bond with Met6929	2.70				
Pi-Alkyl interaction with Leu6898	5.07				
Pi-Alkyl interaction with Met6929	4.09				
Pi-Pi interaction with Tyr6930	5.50				
Pi-Anion interaction with Glu7001	3.44				
Pi-Cation interaction with Lys6968	3.17				
Pi-Cation interaction with Lys6968	3.79				
5	-10.1			Hydrogen bond with Tyr6930	2.27
				Hydrogen bond with Lys6844	1.88
				Non-classical carbon Hydrogen bond with Gly6871	3.52
				Non-classical carbon Hydrogen bond with Asp6897	3.55
		Non-classical carbon Hydrogen bond with Met6929	2.70		
		Pi-Alkyl interaction with Leu6898	4.83		
		Pi-Alkyl interaction with Met6929	4.21		
		Pi-Alkyl interaction with Cys6913	5.49		
		Pi-Pi interaction with Tyr6930	5.5		
		Pi-Anion interaction with Glu7001	3.44		
		Pi-Cation interaction with Lys6968	3.79		
		Pi-Cation interaction with Lys6968	3.12		
		24	-9.9	zHydrogen bond with Lys6968	2.74
				Hydrogen bond with Gly6871	3.34
				Hydrogen bond with Asp6873	2.93
				Non-classical carbon Hydrogen bond with Glu7001	3.72
				Non-classical carbon Hydrogen bond with Tyr6930	3.48
Pi-Alkyl interaction with Leu6898	4.84				
Pi-Alkyl interaction with Tyr6930	5.18				
Pi-Alkyl interaction with Cys6913	4.84				
Pi-Sulfur interaction with Met6929	3.53				

revealing the high dynamic properties of the SARS-COV-2 2'-O-methyltransferase (nsp16), (Figure 7).

The goal of this section is to provide evidence on the stable binding of the proposed inhibitors to nsp16. Based on the proven degrees of flexibility of the binding site of nsp16, simulating the enzyme-inhibitor complex provides a consistent parameter to evaluate its stability upon binding. Thus, it was important to monitor the dynamic behaviour for both SARS-COV-2 2'-O-methyltransferase (nsp16) complex with Sinefungine, and SARS-COV-2 2'-O-methyltransferase (nsp16) complex with compound **11** through measuring the RMSD for both complexes.

RMSD values for both compound **11** and Sinefungine reached at their maximum dynamicity peaks 1.56 Å and 2.25 Å, respectively (Figure 7). This indicates that compound **11** shows better binding to SARS COV-2 2'-O-methyltransferase (nsp16) even more than Sinefungine. Also, it was worthy to monitor the stability of the interactions formed between compound **11** and SARS COV-2

2'-O-methyltransferase (nsp16) through the entire MD experiment. GROMACS has built-in commands that were used to measure the distances of the formed hydrogen bonds between compound **11** and SARS-COV-2 2'-O-methyltransferase (nsp16). The distance between the hydrogen bond donor and the hydrogen bond acceptor in a valid hydrogen bonding should be always less than 3.5 Å. This criterion was fulfilled in all the formed hydrogen bonds between compound **11** and its target indicating a stable and valid mode, (Table 2).

MM-PBSA binding free energy calculations

Another important indicator that gives account for the potential affinity of a ligand with its target is the binding free energy calculated using MM-PBSA and MD calculations. In general, complexes that have lower binding free energy can be considered to be

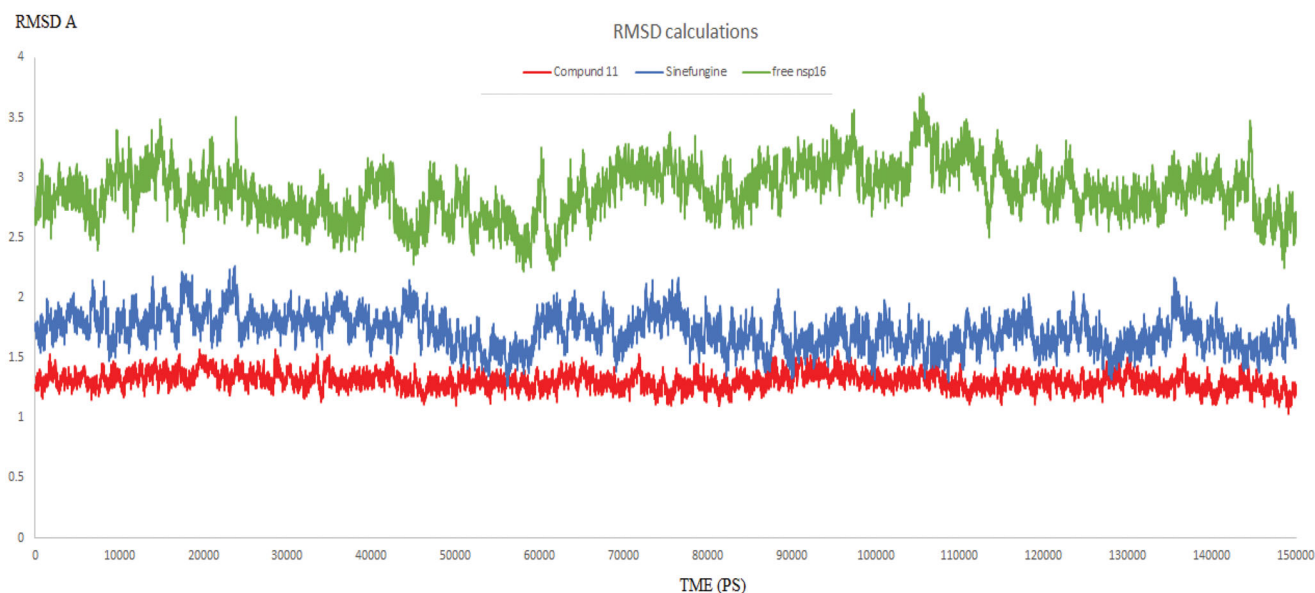


Figure 7. The RMSD of three dynamic simulation experiments. Green colour represents SARS COV-2 2'-O-methyltransferase without a ligand; blue line represents SARS COV-2 2'-O-methyltransferase complex with Sinefungine, and Red line represents SARS COV-2 2'-O-methyltransferase complex with compound 11.

Table 2. The average distances of all the hydrogen bonds formed between compound 11 and SARS COV-2 2'-O-methyltransferase (nsp16) through the entire 150 ns MD simulation.

Hydrogen bond name	Average distance (Å) ± SD
Hydrogen bond with Leu6898	2.37 ± 0.22
Hydrogen bond with Tyr6930	2.41 ± 0.18
Hydrogen bond with Asn6996	1.98 ± 0.09
Hydrogen bond with Glu7001	3.11 ± 0.11

Table 3. The calculated interaction energies and the binding free energy for compound 11 and Sinefungine complexes with SARS COV-2 2'-O-methyltransferase.

Complex	ΔE binding (kJ/mol)	ΔE Electrostatic (kJ/mol)	ΔE Vander Waal (kJ/mol)	ΔE polar solvation (kJ/mol)	SASA (kJ/mol)
Compound 11	-296.95 ± 17.53	-102.82 ± 17.45	-263.40 ± 20.09	98.58 ± 14.92	-23.31 ± 0.99
Sinefungin	-260.86 ± 16.41	-94.13 ± 15.74	-218.08 ± 19.54	71.68 ± 13.97	-20.33 ± 1.04

more stable and their ligands are expected to have high activity and potency. In MD simulation, the binding free energies are calculated for every conformation saved in the trajectory. Accordingly, the *g_mmpbsa* package was used to calculate the MM-PBSA binding free energy for the two complexes of SARS COV-2 2'-O-methyltransferase enzyme with compound 11 and with Sinefungine by the employment of *MmPbSaStat.py* python script. This script brings the package in action to calculate the total free energy for each component of the complex; i.e. the energy of the complex, receptor and the ligand, etc.

Furthermore, the free energy for each component could be calculated by the cumulative sum of its molecular mechanics potential energy in a vacuum and the free energy of solvation. The free energy of solvation includes the polar solvation energy (electrostatic) and nonpolar solvation energy (non-electrostatic), the last one is usually by the solvent accessible surface area (SASA) model. The *g_mmpbsa* package was used to calculate all those types of energies along with the values standard deviation and then summed together to yield the average total free energy of each component. Finally, the binding free energy could be calculated by subtracting the total free energy of the receptor and the total free energy of the ligand from the total free energy of the complex. Table 3 summarises the interaction energies and the binding free energy for the two complexes.

Generally, compound 11–SARS COV-2 2'-O-methyltransferase complex was better than Sinefungine complex in all the calculated energy formats except (polar solvation energy). Its average binding free energy reached -296.95 KJ/mol, while Sinefungine average binding free energy reached -260.86 KJ/mol. The overall results of the three dynamic simulations supported our concept of design and validated the entire virtual screening approach; also, they emphasised the potential inhibitory effect of compound 11 on SARS COV-2 2'-O-methyltransferase.

Conclusion

In the current study we constructed a protocol of structure-based virtual screening aiming at identifying a novel potential inhibitor for SARS COV-2 2'-O-methyltransferase. We used the crystal structure of SARS-COV-2 2'-O-methyltransferase (PDB ID: 6WKQ) in complex with Sinefungine. First, the crystal structure was retrieved from the protein data bank. Then, a 3D pharmacophore model of 4 features and 7 components was constructed based on the binding interactions of Sinefungin with the enzyme. Thereafter, the Zinc database containing 48 Million drug-like compounds was screened through the pharmacophore model. Only 24 compounds were able to pass the pharmacophore filter and were docked

subsequently into the binding site of the enzyme. Compounds (**5**, **9**, **11** and **24**), the best score-ordered hits of the docking result, were selected for further analysis since they exhibited better scores compared to Sinefungin. As a refinement step, we conducted three molecular dynamic simulation experiments for 150 ns. The MD and MM-PBSA outputs revealed compound **11** as the best potential nsp16 inhibitor herein identified, as it displayed a better stability and average binding free energy for the ligand-enzyme complex compared to Sinefungin.

Disclosure statement

No potential conflict of interest was reported by the author(s).

Funding

The authors would like to extend their sincere appreciation to the Deanship of Scientific Research at King Saud University for its funding of this research through the Research Group Project no. RG-1439-065.

References

- Wang M, Cao R, Zhang L, et al. Remdesivir and chloroquine effectively inhibit the recently emerged novel coronavirus (2019-nCoV) in vitro. *Cell Res* 2020;30:269–71.
- Izquierdo L, Helle F, François C, et al. Simeprevir for the treatment of hepatitis C virus infection. *Pharmacogenomics Pers Med* 2014;7:241–9.
- Ramanathan S, et al. Clinical pharmacokinetic and pharmacodynamic profile of the HIV integrase inhibitor elvitegravir. *Clin Pharmacokinet* 2011;50:229–44.
- Chan JF, Yuan S, Kok KH, et al. A familial cluster of pneumonia associated with the 2019 novel coronavirus indicating person-to-person transmission: a study of a family cluster. *Lancet* 2020;395:514–23.
- Boopathi S, Poma AB, Kolandaivel P. Novel 2019 coronavirus structure, mechanism of action, antiviral drug promises and rule out against its treatment. *J Biomol Struct Dyn* 2020;29:1–10.
- Naqvi AA, Fatima K, Mohammad T, et al. Insights into SARS-CoV-2 genome, structure, evolution, pathogenesis and therapies: structural genomics approach. *Biochimica et Biophysica Acta (BBA)-Molecular Basis of Disease* 2020;1866:165878.
- Ziebuhr J. The Coronavirus replicase. In *Coronavirus replication and reverse genetics*. Berlin, Heidelberg: Springer; 2005: 57–94.
- Borgio JF, Alsuwat HS, Al Otaibi WM, et al. State-of-the-art tools unveil potent drug targets amongst clinically approved drugs to inhibit helicase in SARS-CoV-2. *Arch Med Sci* 2020; 16:508–18.
- Li G, De Clercq E. Therapeutic options for the 2019 novel coronavirus (2019-nCoV). *Nature Reviews. Drug Discovery* 2020;19:149–50. <https://pubchem.ncbi.nlm.nih.gov/compound/92727>
- Jeong GU, Song H, Yoon GY, et al. Therapeutic Strategies Against COVID-19 and structural characterization of SARS-CoV-2: a review. *Front Microbiol* 2020;11:1723.
- Chen Y, Guo D. Molecular mechanisms of coronavirus RNA capping and methylation. *Viol Sin* 2016;31:3–11.
- Krafcikova P, Silhan J, Nencka R, et al. Structural analysis of the SARS-CoV-2 methyltransferase complex involved in RNA cap creation bound to sinefungin. *Nat Commun* 2020;11: 3717.
- Ramanathan A, Robb GB, Chan SH. mRNA capping: biological functions and applications. *Nucleic Acids Res* 2016; 44:7511–26.
- Daffis S, Szretter KJ, Schriewer J, et al. 2'-O methylation of the viral mRNA cap evades host restriction by IFIT family members. *Nature* 2010;468:452–6.
- El Hassab MA, Shoun AA, Al-Rashood ST, et al. Identification of new potential Covid-19 polymerase inhibitor via combining fragment-based drug design, docking, molecular dynamics and MM-PBSA calculations. *Front Chem* 2020;8:584894.
- Case DA, Cheatham TE, 3rd, Darden T, et al. The Amber biomolecular simulation programs. *J Comput Chem* 2005;26: 1668–88.
- Vilar S, Cozza G, Moro S. Medicinal chemistry and the Molecular Operating Environment (MOE): application of QSAR and molecular docking to drug discovery. *Curr Top Med Chem* 2008;8:1555–72.
- Valasani KR, Vangavaragu JR, Day VW, Yan SS. Structure based design, synthesis, pharmacophore modeling, virtual screening, and molecular docking studies for identification of novel cyclophilin D inhibitors. *J Chem Inf Model* 2014;54: 902–12.
- Wei Y, Li J, Qing J, et al. Discovery of novel hepatitis C virus NS5B polymerase inhibitors by combining random forest, multiple pharmacophore modeling and docking. *PLoS One* 2016;11:e0148181.
- Trott O, Olson AJ. AutoDock vina: improving the speed and accuracy of docking with a new scoring function, efficient optimization, and multithreading. *J Comput Chem* 2010;31: 455–61.
- Morris GM, Huey R, Lindstrom W, et al. Autodock4 and AutoDockTools4: automated docking with selective receptor flexibility. *J. Comput Chem* 2009;30:2785–91. 2009
- Available from: <https://3dsbiovia.com/resource-center/downloads/>
- Abraham MJ, Murtola T, Schulz R, et al. GROMACS: high performance molecular simulations through multi-level parallelism from laptops to supercomputers. *SoftwareX* 2015;1–2: 19–25.
- Phillips JC, Braun R, Wang W, et al. Scalable molecular dynamics with NAMD. *J Comput Chem* 2005;26:1781–802.
- Chiu SW, Pandit SA, Scott HL, Jakobsson E. An improved united atom force field for simulation of mixed lipid bilayers. *J Phys Chem B* 2009;113:2748–63.
- Bhardwaj VK, Singh R, Sharma J, et al. Identification of bio-active molecules from Tea plant as SARS-CoV-2 main protease inhibitors. *J Biomol Struct Dyn* 2020;8:1–13.
- Kumari R, Kumar R, Lynn A. Open source drug discovery and A. Lynn. *J Chem Inf Model* 2014;54:1951–62.
- Alamri MA, Tahir ul Qamar M, Mirza MU, et al. Pharmacoinformatics and molecular dynamics simulation studies reveal potential covalent and FDA-approved inhibitors of SARS-CoV-2 main protease 3CLpro. *J Biomol Struct Dyn* 2020;23:1–3.
- El-Hasab MA, El-Bastawissy EE, El-Moselhy TF. Identification of potential inhibitors for HCV NS3 genotype 4a by combining protein-ligand interaction fingerprint, 3D

- pharmacophore, docking, and dynamic simulation. *J Biomol Struct Dyn* 2018;36:1713–27.
30. El-Hassab MAE, El-Bastawissy EE, El-Moselhy TF. Identification of potential inhibitors for HCV NS5b of genotype 4a by combining dynamic simulation, protein-ligand interaction fingerprint, 3D pharmacophore, docking and 3D QSAR. *J Biomol Struct Dyn* 2020;38:4521–35.
 31. Nagarajan H, Narayanaswamy S, Vetrivel U. Mutational landscape screening of methylene tetrahydrofolate reductase to predict homocystinuria associated variants: an integrative computational approach. *Mutat Res* 2020;819–820: 111687–820.
 32. Chen S, Wiewiora RP, Meng F, et al. The dynamic conformational landscape of the protein methyltransferase SETD8. *Elife* 2019;8:e45403.
 33. Xiao B, Jing C, Kelly G, et al. Specificity and mechanism of the histone methyltransferase Pr-Set7. *Genes Dev* 2005;19: 1444–54.